PNAS RESEARCH ARTICLE | MICROBIOLOGY OPEN ACCESS

Sulfur and methane oxidation by a single microorganism

Joo-Han Gwak[a,1], Samuel Imisi Awala[a,1], Ngoc-Loi Nguyen[a], Woon-Jong Yu[a], Hae-Young Yang[a], Martin von Bergen[b,c], Nico Jehmlich[b], K. Dimitri Kits[d], Alexander Loy[d], Peter. F. Dunfield[e], Christiane Dahl[f], Jung-Ho Hyun[g], and Sung-Keun Rhee[a,2]

Edited by Donald Canfield, Syddansk Universitet, Odense M., Denmark; received August 17, 2021; accepted June 22, 2022

Natural and anthropogenic wetlands are major sources of the atmospheric greenhouse gas methane. Methane emissions from wetlands are mitigated by methanotrophic bacteria at the oxic–anoxic interface, a zone of intense redox cycling of carbon, sulfur, and nitrogen compounds. Here, we report on the isolation of an aerobic methanotrophic bacterium, '*Methylovirgula thiovorans*' strain HY1, which possesses metabolic capabilities never before found in any methanotroph. Most notably, strain HY1 is the first bacterium shown to aerobically oxidize both methane and reduced sulfur compounds for growth. Genomic and proteomic analyses showed that soluble methane monooxygenase and XoxF-type alcohol dehydrogenases are responsible for methane and methanol oxidation, respectively. Various pathways for respiratory sulfur oxidation were present, including the Sox–rDsr pathway and the S_4I system. Strain HY1 employed the Calvin–Benson–Bassham cycle for CO_2 fixation during chemolithoautotrophic growth on reduced sulfur compounds. Proteomic and microrespirometry analyses showed that the metabolic pathways for methane and thiosulfate oxidation were induced in the presence of the respective substrates. Methane and thiosulfate could therefore be independently or simultaneously oxidized. The discovery of this versatile bacterium demonstrates that methanotrophy and thiotrophy are compatible in a single microorganism and underpins the intimate interactions of methane and sulfur cycles in oxic–anoxic interface environments.

facultative methanotrophy | thiotrophy | mixotrophy | wetland

Significance

Wetlands are the major natural source of methane, an important greenhouse gas. The sulfur and methane cycles in wetlands are linked—e.g., a strong sulfur cycle can inhibit methanogenesis. Although there has historically been a clear distinction drawn between methane and sulfur oxidizers, here, we isolated a methanotroph that also performed respiratory oxidization of sulfur compounds. We experimentally demonstrated that thiotrophy and methanotrophy are metabolically compatible, and both metabolisms could be expressed simultaneously in a single microorganism. These findings suggest that mixotrophic methane/sulfur-oxidizing bacteria are a previously overlooked component of environmental methane and sulfur cycles. This creates a framework for a better understanding of these redox cycles in natural and engineered wetlands.

Atmospheric methane (CH_4) is a potent greenhouse gas responsible for about 15% of the total greenhouse effect (1). The amount of CH_4 in Earth's atmosphere is gradually increasing (2). The world's largest single CH_4 source is natural wetlands, one-third of which are temperate and boreal northern wetlands (3, 4). Methane produced by the degradation of organic matter in anoxic sediments reaches the atmosphere via diffusion, transport through aerenchymous roots, or ebullition. Much of the diffusive flux of CH_4 is oxidized by aerobic methanotrophic bacteria at oxic–anoxic interfaces in wetlands, thereby limiting CH_4 emission (5–8). Methane formation is also prevented by the activity of microorganisms that redirect the flow of electrons and carbon away from methanogenic archaea, such as certain sulfur-cycling microorganisms. Microorganisms that respire sulfate (SO_4^{2-}) or other oxidized sulfur compounds can contribute considerably to the anaerobic degradation of organic carbon in wetlands and outcompete methanogenic archaea (9, 10).

Aerobic methanotrophic bacteria were long assumed to have a limited substrate spectrum, including methane, methanol, and occasionally other C1 compounds, but no other substrates (11). This assumption was overturned when it was discovered that methanotrophs of the genus *Methylocella* (family Beijerinckiaceae) use some simple organic acids, alcohols, and short-chain alkanes as alternative substrates to methane (11, 12). A few other alphaproteobacterial methanotrophs belonging to the Methylocystaceae or Beijerinckiaceae families, while not as versatile as *Methylocella*, have also been shown to metabolize acetate and/or ethanol (13–15). Two cultured Beijerinckiaceae methanotrophs even possess the genetic capacity for aerobic CO oxidation (16, 17), and the growth of one of them, '*Methylocapsa gorgona*' MG08, was supported by CO in the presence of methane (18). In addition, thermophilic and mesophilic verrucomicrobial methanotrophs of the proposed genera '*Methylacidiphilum*' and '*Methylacidimicrobium*' grow autotrophically on CO_2 with H_2 as an electron donor (19–23). In fact, genes encoding NiFe hydrogenase are widespread in all major taxonomic families of methanotrophs, suggesting that H_2 may be a common supplemental energy source for these bacteria in nature. Recently, members of the genus *Methylacidiphilum* were also found to grow heterotrophically on various C3 compounds (24). Clearly, some methanotrophs can take advantage of other small-molecule substrates besides methane and methanol, which may enhance their survival and/or growth in natural habitats where CH_4 concentrations are low and/or variable (13).

Author contributions: J.-H.G., S.I.A., N.-L.N., and S.-K.R. designed research; J.-H.G., S.I.A., N.-L.N., W.-J.Y., H.-Y.Y., M.v.B., and N.J. performed research; J.-H.G., S.I.A., N.-L.N., W.-J.Y., N.J., K.D.K., C.D., J.-H.H., and S.-K.R. analyzed data; and J.-H.G., S.I.A., K.D.K., A.L., P.F.D., C.D., and S.-K.R. wrote the paper.

The authors declare no competing interest.

This article is a PNAS Direct Submission.

[1]J.-H.G. and S.I.A. contributed equally to this work.

[2]To whom correspondence may be addressed. Email: rhees@chungbuk.ac.kr.

This article contains supporting information online at http://www.pnas.org/lookup/suppl/doi:10.1073/pnas.2114799119/-/DCSupplemental.

Published August 1, 2022.

The oxidation of H_2 to two protons and the oxidation of CO to CO_2 both yield considerably lower standard free-energy changes, $\Delta G^{\circ\prime} = -237$ kJ·mol^{-1} H_2 and $\Delta G^{\circ\prime} = -249$ kJ·mol^{-1} CO, respectively, than the complete oxidation of CH_4 to CO_2 ($\Delta G^{\circ\prime} = -818$ kJ·mol^{-1} CH_4). In comparison, the standard free-energy changes for the oxidation of H_2S to SO_4^{2-} ($\Delta G^{\circ\prime} = -797$ kJ·mol^{-1} H_2S) and $S_2O_3^{2-}$ to SO_4^{2-} ($\Delta G^{\circ\prime} = -818$ kJ·mol^{-1} $S_2O_3^{2-}$) are similar to that for CH_4 oxidation. Based on these considerations, reduced sulfur compounds would be well-suited alternative substrates for methanotrophs.

To date, there has been a clear distinction between thiotrophic and methanotrophic microorganisms. The growth of methanotrophs using reduced sulfur compounds as electron donors has never been reported. Recently, a member of the genus *Methylacidiphilum* was found to degrade methanethiol and sulfide for detoxification, but no growth benefit was observed from their oxidation (25). The common occurrence of *sqr* (encoding sulfide: quinone oxidoreductase) (Fig. 1) and *mtoX* (encoding methanethiol oxidase) (25) in methanotroph genomes suggests that detoxification mechanisms are common. However, genomes of some methanotrophs also harbor a complete Sox system (Dataset S1 and Fig. 1), and a recent study unveiled the co-occurrence of genes encoding sulfur (Sox and reverse dissimilatory sulfite reductase [rDsr]) and CH_4 (methane monooxygenase) oxidation systems in a metagenome-assembled genome recovered from a permafrost thaw wetland (26). These findings provide hints for a possible combination of thiotrophy and methanotrophy in particular bacteria. Here, we experimentally confirmed this hypothesis and isolated a facultative methanotroph (strain HY1) that harbors a complete repertoire of sulfur oxidation genes encoding the Sox–rDsr system (without *soxCD*).

Results and Discussion

Isolation of Methanotrophic Strain HY1. Wetland samples were incubated at pH 4.0 in a low-salt mineral (LSM) medium under methanotrophic conditions. From a methane-oxidizing enrichment culture transferred biweekly for about 6 mo, colonies of methanotrophs were retrieved by using a floating filter technique. A methanotrophic isolate designated HY1 showed 98.7% 16S ribosomal RNA (rRNA) gene-sequence identity to *Methylovirgula ligni* within the family Beijerinckiaceae in the order Hyphomicrobiales (*SI Appendix*, Fig. S1). Culture purity was verified via Illumina sequencing of a 16S rRNA gene amplicon, as well as via full genome sequencing and assembly. The average nucleotide identity value for the genome of strain HY1 was 73.6% with that of *M. ligni* and ranged from 72.2 to 73.6% with selected members of the Beijerinckiaceae, indicating that the isolate represents a novel species of the genus *Methylovirgula*. Growth was observed at moderate temperature in an acidic pH range between pH 4 and 6 and an optimum at pH 4.5 on methanol (*SI Appendix*, Fig. S2), similar to other methanotrophic members of the Beijerinckiaceae (*SI Appendix*, Table S1).

Thiotrophic Growth. Previously isolated strains of *Methylovirgula* are methylotrophs that cannot oxidize CH_4 as an energy source (27), although they are closely related phylogenetically to the methanotrophic genera *Methylocella* and *Methyloferula* within the Beijerinckiaceae (28) (Fig. 1 and *SI Appendix*, Fig. S1). Strain HY1 was observed in batch culture to grow on methane as well as various C1–C4 alcohols, organic acids, and short-chain alkanes (Table 1). This substrate range is similar to

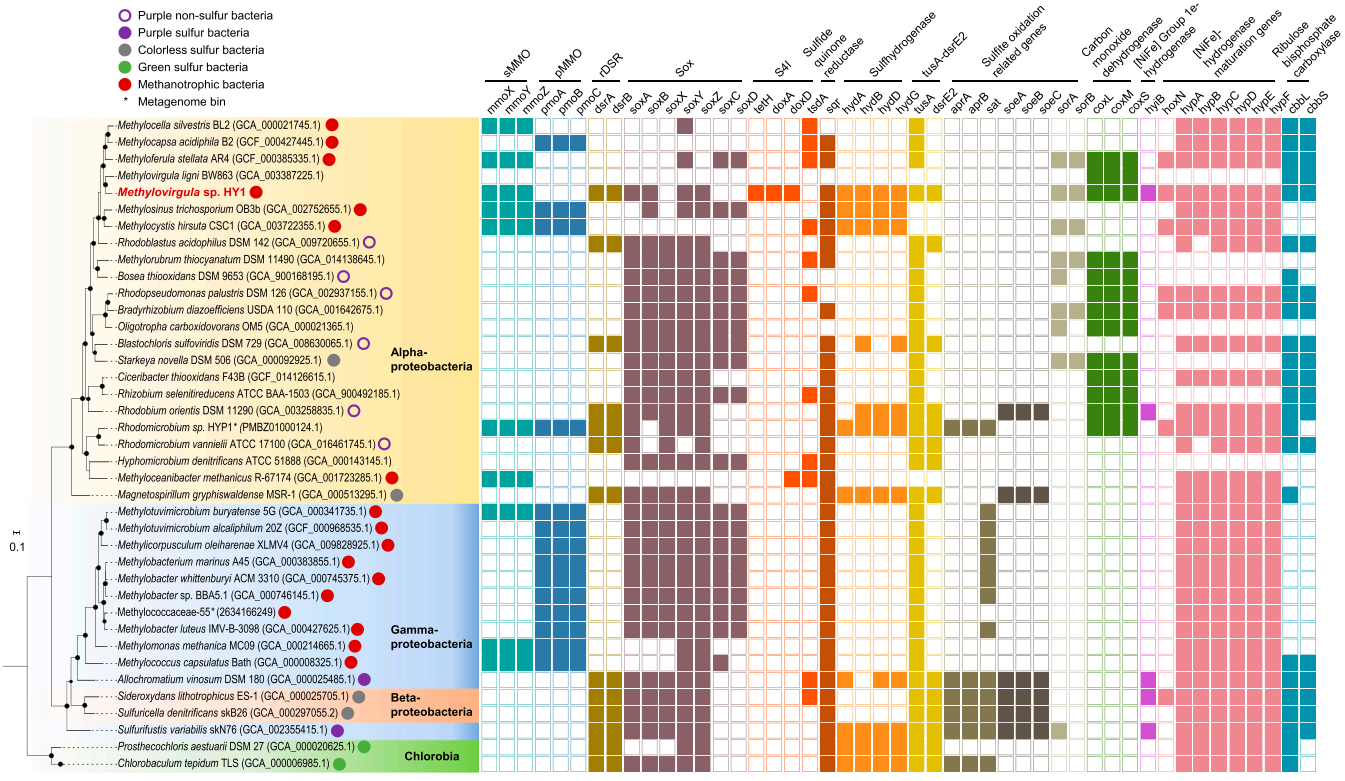

Fig. 1. Phylogenomic tree and distribution of distinctive metabolic traits in methane- and sulfur-oxidizing bacteria in the classes Alphaproteobacteria, Betaproteobacteria, Gammaproteobacteria, and Chlorobia. The tree includes 37 genomes and 2 metagenome-assembled genomes. Representative genomes of Sox-containing Alphaproteobacterial and Gammaproteobacterial methanotrophs were included. The tree was constructed based on 27 concatenated ribosomal proteins with FastTree implemented within Anvi'o phylogenomics workflow (details are in *Materials and Methods*). Black circles indicate 70% bootstrap support for nodes along the tree. A homology-based search for functional genes was performed by using BLAST (124), OrthoFinder (125), and manual examination (details are in *Materials and Methods*). Solid and open squares indicate the presence and absence of the genes, respectively.

Table 1. Substrate utilization by strain HY1

Substrate	Concentration	Growth		
		Strain HY1	*M. silvestris* BL2	*M. ligni* BW863
Organic				
C1				
Methane	2.5 to 20%	++	++	–
Methanol	20 mM	++	++	++
Formate	5 mM	+	+	–
Formate	20 mM	–	++	–
C2				
Ethane	2.5 to 20%	++	++	–
Ethanol	5 mM, 20 mM	+	+	+
Acetate	5 mM	+	++	–
Acetate	20 mM	–	–	–
Oxalate	5 mM	++	–	–
Oxalate	20 mM	+	–	–
C3				
Propane	2.5%	+	++	–
Propane	20%	–	++	–
1-Propanol	5 mM	+	–	–
1-Propanol	20 mM	–	–	–
2-Propanol	5 mM	+	++	–
2-Propanol	20 mM	+	++	–
1,2-Propanediol	5 mM, 20 mM	++	++	–
Acetone	5 mM	++	++	–
Acetone	20 mM	+	+	–
Acetol	5 mM	++	++	–
Acetol	20 mM	+	++	–
Pyruvate	5 mM	–	++	+
Pyruvate	20 mM	+	++	++
C4				
Butane	2.5%	+	–	–
Butane	20%	–	–	–
1-Butanol	5 mM	++	–	–
1-Butanol	20 mM	–	–	–
2-Butanol	5 mM	++	–	–
1-Butanol	20 mM	–	–	–
Butanal	5 mM	++	–	–
Butanal	20 mM	+	–	–
2-Butanone	5 mM	++	–	–
2-Butanone	20 mM	+	–	–
Succinate	5 mM	+	++	–
Succinate	20 mM	++	++	–
Malate	5 mM	+	+	+
Malate	20 mM	++	++	++
Inorganic				
Sulfur*				
Thiosulfate	1 mM	+	–	–
Thiosulfate	15 mM	+	–	–
Tetrathionate	2 mM	+	–	–
Elemental sulfur (S°)	3 g/L	+	–	–
Others				
H_2	20%	–	–	–
CO	20%	–	–	–

Each substrate tested was supplied as a sole energy source to batch cultures. Growth is indicated as follows: ++, growth to $OD_{600} > 0.25$; +, growth to $OD_{600} \geq 0.04$ to 0.25; –, growth to $OD_{600} < 0.04$. All the substrates were tested with 5% CO_2. *M. silvestris* BL2 and *M. ligni* BW863 were retested in parallel to strain HY1, and the results largely conformed to previous reports (11, 12, 29, 30). Accumulation of sulfate was also used as an indicator of biological sulfur oxidation.
*Due to rapid autoxidation of sulfide in our condition (126, 127), growth on sulfide could not be tested. Instead, a microrespirometry experiment was performed to show the oxidation of sulfide by strain HY1 by using high-density cells (Table 2).

facultative methanotrophs of the genus *Methylocella* (Table 1) (11, 12, 29, 30), which show 95.8 to 96.3% 16S rRNA gene-sequence similarity with strain HY1.

Surprisingly, strain HY1 also grew on the inorganic sulfur compounds thiosulfate, tetrathionate, and elemental sulfur (S°), a capability never before observed in any methanotroph (Table 1). Because growth of a single organism on methane and reduced sulfur was an unprecedented observation, these processes were carefully verified by time-course analysis of batch cultures using analytical methods described in *SI Appendix, Analytical Methods*.

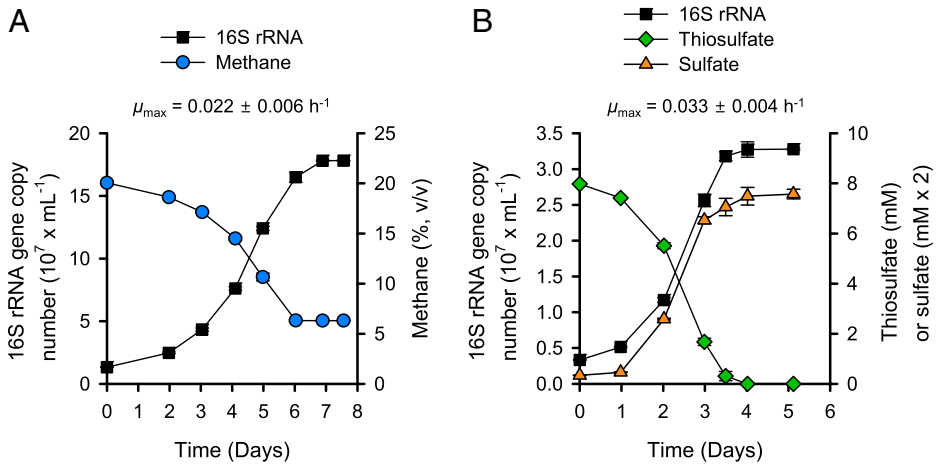

Fig. 2. Growth and time course of methane and thiosulfate oxidation by batch cultures of strain HY1. (*A*) Time courses of methane oxidation and the concomitant growth of strain HY1. Due to oxygen depletion, methane was not completely oxidized. (*B*) Time courses of thiosulfate oxidation, sulfate production, and the concomitant growth of strain HY1. The stoichiometry of thiosulfate consumption to sulfate production was nearly equal to the predicted 1:2. Specific analytical assays for methane, sulfate, and thiosulfate in batch cultures are described in *SI Appendix, Analytical Methods*. Error bars represent ±1 SD of three biological replicates. V/v, vol/vol.

Consumption of methane or thiosulfate as sole growth substrates and production of sulfate from thiosulfate were observed concurrent with population growth (Fig. 2). A near-stoichiometric conversion of thiosulfate to sulfate at 1:1.98 was observed when low thiosulfate concentrations (<5 mM) were added (Eq. **1**) (Fig. 2*B*).

$$S_2O_3^{2-} + 2\,O_2 + H_2O \rightarrow\ 2\ SO_4^{2-} + 2H^+. \qquad [1]$$

Abiotic decomposition of thiosulfate was observed only at pH < 3.0 (*SI Appendix*, Fig. S3). In this study, strain HY1 was cultivated in a buffered medium at pH 4.5 to 5.0, and abiotic decomposition of thiosulfate was therefore assumed to be negligible.

An increase in 16S rRNA gene copies during the oxidation of methane or thiosulfate indicated that both substrates supported population growth (Fig. 2). Biomass production was also demonstrated via quantification of cellular protein in the cultures and measurement of molar growth yield $Y_{x/m}$ (g dry cell weight·mol^{-1} substrate) (Fig. 3). Furthermore, methane and thiosulfate were oxidized concomitantly when both substrates were provided simultaneously (*SI Appendix*, Fig. S4). Accordingly, the biomass produced when methane and thiosulfate were simultaneously used was almost equal to the sum of the biomass produced when a similar amount of methane and thiosulfate was utilized individually (Fig. 3*A*). The biomass molar growth yields ($Y_{x/m}$) were comparable between methane- and thiosulfate-grown cells (Fig. 3*B*), as expected from the similar standard free-energy changes for their oxidations (introduction).

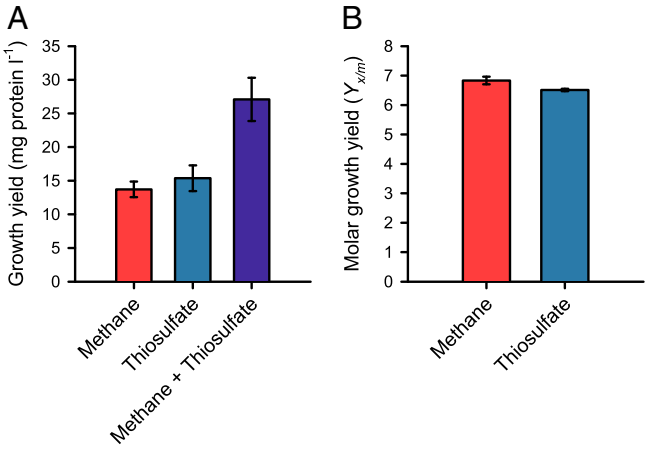

Fig. 3. Biomass production in strain HY1 grown on methane and thiosulfate. (*A*) The growth yield was calculated as milligrams of cellular protein produced per culture volume (mg·protein·L^{-1}) after the complete oxidation of the substrate(s). Strain HY1 was grown in 100 mL of LSM medium at pH 5.0 with methane (15%, vol/vol), thiosulfate (4 mM), and methane+thiosulfate (15%, vol/vol; 4 mM), respectively, in 160-mL serum vials. For the complete oxidation of substrates, 60% (vol/vol) oxygen was supplied. (*B*) The molar growth yield ($Y_{x/m}$) was calculated as gram of dry cell weight per mol of substrate consumed (g dry cell weight·mol^{-1}·substrate). Error bars represent ±1 SD of three biological replicates.

Genomic Properties. The observed capacity of strain HY1 to grow on both methane and reduced sulfur compounds prompted us to investigate the genomic basis for these processes. The final assembled genome contained two circular contigs: a circular chromosome and a 278-kb circular megaplasmid. The overall genomic features of strain HY1 compared with other methanotrophs in the Beijerinckiaceae are presented in *SI Appendix*, Table S1. The most surprising finding from the genomic analysis was the identification of a comprehensive genetic repertoire encoding the utilization of reduced sulfur compounds as electron donors (Fig. 1 and Datasets S1 and S2). The assembly verified the presence of genes encoding methane oxidation and sulfur oxidation within a single organism's genome.

Genes encoding for methane and short-chain alkane oxidation. The key genes encoding CH_4 oxidation predicted from the genomic analysis are presented in Dataset S2, and the predicted pathways for methane oxidation are presented in Fig. 4. While a gene cluster for sMMO, a soluble diiron monooxygenase family enzyme (31), is present, genes for particulate methane monooxygenase (pMMO) are absent. The genes encoding sMMO, *mmoXYBZDC*, are closely related phylogenetically to those of other methanotrophs possessing only sMMO, such as *Methylocella*, *Methyloferula*, and *Methyloceanibacter* (32, 33), and the gene arrangements are highly conserved among these methanotrophs (*SI Appendix*, Fig. S5).

Another key genomic trait of strain HY1 is the absence of genes encoding Ca^{2+}-dependent methanol dehydrogenase (MDH) or PQQ-dependent alcohol dehydrogenase. Instead, strain HY1 contains four genes encoding lanthanide-dependent MDH (XoxF-type MDH) affiliated with the XoxF3 and XoxF5 clades (34) (*SI Appendix*, Table S2). Consistent with this finding, strain HY1 could not grow on methane or methanol without the addition of lanthanides to the medium (*SI Appendix*, Fig. S6).

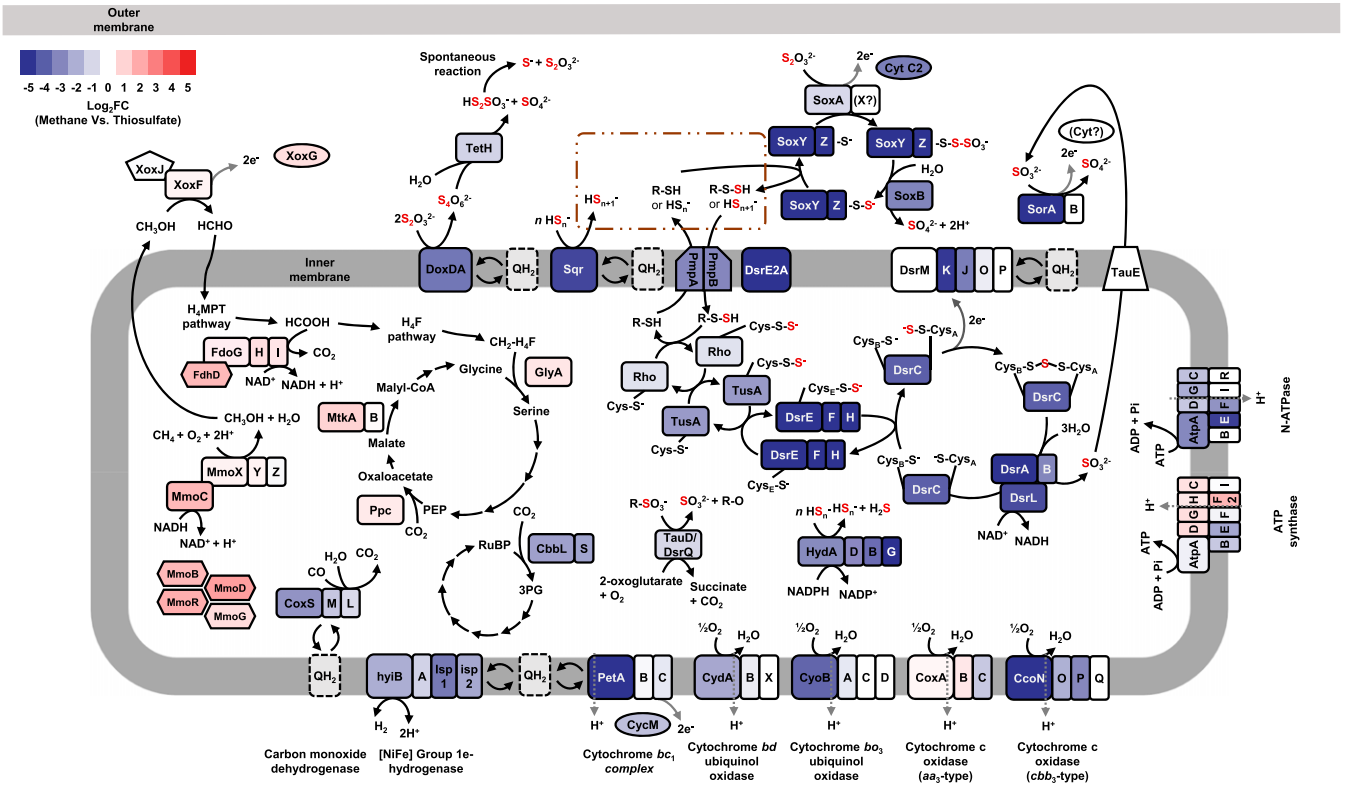

Fig. 4. Proposed central carbon and energy metabolism in strain HY1 and differential protein abundance between methane-grown and thiosulfate-grown cells. The color scale indicates whether proteins have higher abundance in methane-grown (red) or thiosulfate-grown (blue) cells. The intensity of the color in each protein indicates the relative fold change difference (log_2FC). Methane oxidation: Methane is oxidized to methanol by the soluble methane monooxygenase, sMMO (MHY1_02902–2908). The produced methanol is oxidized to formaldehyde via the lanthanide-dependent MDH, XoxF (MHY1_02202 was the most abundant MDH). Formaldehyde oxidation to formate then proceeds via the tetrahydromethanopterin (H_4MPT) pathway, and C1 incorporation into the serine cycle is mediated by the tetrahydrofolate (H_4F) carbon-assimilation pathway. Sulfur oxidation: In the periplasm, two thiosulfate molecules are oxidized to tetrathionate by thiosulfate dehydrogenase, DoxDA (MHY1_01298), and then TetH (MHY1_02468) hydrolyzes tetrathionate to sulfate and disulfane monosulfonic acid, which most probably decomposes spontaneously to thiosulfate and sulfur. Sulfane sulfur derived from thiosulfate and sulfide via SoxYZAB (MHY1_00063–66) and Sqr (MHY1_02376), respectively, is transported into the cytoplasm via PmpAB (MHY1_00234–235 and MHY1_01361–1362; only MHY1_01361–1362 are indicated here), then transferred to the DsrEFH (MHY1_00081–83) and DsrC (MHY1_00084) via the sulfur-transporting complex [rhodanese (MHY1_01281)-TusA (MHY1_00072)-DsrE2A (MHY1_00073)]. The persulfurated DsrC is oxidized to DsrC and sulfite by DsrAB sulfite reductase (MHY1_00079–80), thereby releasing electrons to the iron–sulfur flavoprotein, DsrL (MHY1_00087). Sulfite is probably transported to the periplasm by a TauE-like exporter (MHY1_01299). The sulfite:cytochrome *c* oxidoreductase, SorAB (MHY1_p00095–0096), encoded in the megaplasmid, might be involved in sulfite oxidation. It is speculated that the TauD/DsrQ protein (MHY1_00078) catalyzes the release of sulfite during the breakdown of sulfonates.

Aside from the verrucomicrobial methanotrophs (35–37), strains PC1 and PC4 of *Methylocella tundrae* have been reported to contain only XoxF-type MDH and are dependent on lanthanides for their growth (30). The tetrahydromethanopterin (H_4MPT) pathway for formaldehyde oxidation to formate and the tetrahydrofolate (H_4F) pathway mediating C1 transfer to the serine cycle, which are widely conserved in Beijerinckiaceae methanotrophs, are both encoded in strain HY1 (Dataset S2).

Strain HY1 also utilized butane (2.5%, volume [vol]/vol) and its possible catabolic intermediates (i.e., l-butanol and isobutanol) (Table 1), which is unique among known methanotrophs (29). *Methylocella silvestris* BL2 is equipped with genes encoding two different soluble diiron monooxygenase family enzymes—i.e., sMMO and propane monooxygenase—and can utilize C_1–C_3 alkanes for growth (12). In contrast, the genome of strain HY1 encodes a single diiron monooxygenase, sMMO. Nevertheless, it cannot only grow on C_1–C_3 alkanes, but also on butane (C_4). Notably, the dedicated propane monooxygenase from *M. silvestris* BL2 requires high propane concentrations (20%, vol/vol) (Table 1). Thus, the absence of a related propane monooxygenase may explain why strain HY1 utilizes propane (and butane) only when provided at low concentrations (2.5%, vol/vol). We hypothesize that the single sMMO in strain HY1 has a broad substrate range, including butane, and initiates oxidation of various short-chain alkanes to both primary and secondary alcohols, as reported for other soluble methane monooxygenases (38–40). The growth of strain HY1 on various alcohols is likely attributable to the presence of a repertoire of various XoxF-type MDHs with potential broad substrate specificity (*SI Appendix*, Table S2) (37, 41–43). The enzymes required to oxidize the ketones derived from secondary alcohols remain elusive (44–47). The complete set of genes encoding for the tricarboxylic acid cycle in strain HY1 (Dataset S2) is a common trait of alphaproteobacterial methanotrophs (48), but is also consistent with strain HY1's utilization of multicarbon compounds.

Genes encoding for oxidation of reduced sulfur compounds. A repertoire of genes encoding enzymes involved in sulfur oxidation (*soxYZAB*, *dsrABEFHCMKLJOPN*, *sqr*, *sorAB*, *tetH*, and *doxAD*) suggested that strain HY1 is capable of using various reduced sulfur compounds for growth (Fig. 1 and Dataset S2). Predicted pathways of sulfur oxidation are summarized in Fig. 4 and described in detail below.

In strain HY1, the *sox*, *dsr*, and other genes form a single gene cluster (*SI Appendix*, Fig. S7). The combination of a periplasmic, truncated Sox system, which lacks SoxCD, with a cytoplasmic rDsr system in strain HY1 is widespread in bacterial sulfur oxidizers and occurs in at least four class-level lineages, including Alphaproteobacteria, Betaproteobacteria, Gammaproteobacteria,

and Chlorobia (Fig. 1). Many organisms containing these genes, such as green and purple anoxygenic phototrophic sulfur bacteria, form sulfur deposits as a characteristic intermediate en route to the end-product sulfate (49–51).

The oxidation of reduced sulfur compounds—e.g., thiosulfate, sulfide, or polysulfides—to sulfate is always initiated in the periplasm, and we can confidently state that the SoxAYZAB proteins in strain HY1 constitute a periplasmic multienzyme system (Fig. 4). SoxYZ serves as a carrier protein to which reduced sulfur compounds remain attached during the oxidation process. SoxA(X) catalyzes the oxidative fusion of the sulfur substrate (e.g., thiosulfate) to a conserved cysteine of SoxY. A gene encoding SoxX was not found in the genome of strain HY1, as has been reported for the sulfur oxidizers *Halomonas halophila* and *Beggiatoa* sp. PS (52). In classical heterodimeric SoxAX proteins, the *c*-type cytochrome SoxX serves as the site of electron storage and transfer to an electron-transfer partner cytochrome *c* during turnover of the enzyme, while SoxA harbors the catalytically active site (52). It is therefore conceivable for strain HY1 that SoxA alone is active and that it transfers electrons directly to a separate *c*-type cytochrome acceptor encoded elsewhere in the genome. Similar observations have been made for thiosulfate dehydrogenase, where the encoding gene *tsdA* is accompanied by the gene *tsdB* for the electron-accepting cytochrome *c* in many, but not in all, TsdA-containing organisms (53). Once thiosulfate is bound to SoxYZ, the sulfone group ($-SO_3^-$) is hydrolytically released by SoxB. The SoxB of strain HY1 is related phylogenetically to other alphaproteobacterial SoxB proteins (*SI Appendix*, Fig. S8) and shows the closest affiliation to the enzymes from known sulfide- and/or thiosulfate-oxidizing organisms of the order Hyphomicrobiales, including aerobic members of the genus *Magnetospirillum* (54).

Other alphaproteobacterial methanotrophs that contain *soxB* are *Methylosinus trichosporium* OB3b (55) and *Methylosinus* sp. 3S-1 (56), but additional components of the Sox machinery (SoxA and SoxX) are not encoded in these organisms (Dataset S1). Thus, it is unlikely that they can oxidize thiosulfate. A complete Sox system containing a SoxCD has been reported in genomes of the gammaproteobacterial methanotroph genera *Methylotuvimicrobium*, *Methylicorpusculum*, *Methylobacter*, and *Methylosarcina*, but their potential for sulfur oxidation has not been experimentally proven (Dataset S1). *Methylicorpusculum oleiharenae* XLMV4 could not be grown on thiosulfate compounds, despite possessing a complete Sox system (57). The lack of a potential redox-active motif (CxxxC) in SoxD of methanotrophs (*SI Appendix*, Fig. S9) implies that it might be nonfunctional or has a different metabolic function (58, 59). In that case, they would need an auxiliary system, such as the rDsr or Hdr (heterodisulfide reductase)-like system, for sulfur oxidation to sulfite. Strain HY1 encodes rDsr, but these enzymes are not encoded in any other methanotroph genomes presently available (Dataset S1).

As the genome of HY1 does not encode sulfane dehydrogenase SoxCD, sulfane sulfur atoms ($-S^-$) bound to SoxYZ cannot be further oxidized in the periplasm. The described attachment of thiosulfate and release of sulfate likely repeats, and chains of sulfur atoms are formed that probably lead to the intermediary formation of sulfur deposits. Two other enzyme systems can also contribute to sulfur formation. Strain HY1 encodes enzymes of the so-called S_4 intermediate (S_4I) pathway that act on thiosulfate in the periplasm (Fig. 4): Two thiosulfate molecules are first oxidized to tetrathionate by thiosulfate dehydrogenase (DoxDA), and then tetrathionate hydrolase (TetH) hydrolyzes tetrathionate to sulfate and disulfane monosulfonic acid, which probably decomposes spontaneously to thiosulfate and sulfur (60, 61). In addition, gene MHY1_02376 encodes a type I Sqr, a periplasmically oriented monotopic membrane protein catalyzing the oxidation of sulfide and probably releasing hydrophilic polysulfides that can also contribute to sulfur deposition (Fig. 4) (62, 63).

In the next step, sulfur formed either via the Sox or S_4I pathways or resulting from the action of Sqr is transferred into the cytoplasm (Fig. 4). How this is achieved in general by sulfur oxidizers is unclear. A YeeE/YedE protein resembling the thiosulfate transporter from *Escherichia coli* and *Spirochaeta thermophila* (64) is possibly involved in the process in *Hyphomicrobium denitrificans*. However, this organism does not contain Dsr proteins (65). Strain HY1 does not encode a full-length YeeE/YedE homolog; instead, two sets of *pmpA* and *pmpB* homologous genes are present (MHY1_00234–235 and MHY1_01361–1362). PmpAB conform to the first third of the YeeE/YedE domain and have also been discussed as potential transport components for sulfur-containing compounds (66). Notably, a gene encoding a periplasmic DsrE-like sulfurtransferase (MHY1_00068) resides in the *sox* operon of strain HY1, and a membrane-bound DsrE-like sulfurtransferase (MHY1_00073) is encoded in the immediate vicinity, between the *sox* and *dsr* clusters. We consider the possibility that the first may be involved in sulfur transfer to the latter, which may then mediate transport of the sulfur into the cytoplasm.

Inside the cytoplasm, sulfur never occurs in free form, but is handled by further sulfurtransferases, such as TusA (MHY1_00072) and DsrEFH (MHY1_00081–83), and treated by the concerted action of *dsr*-encoded enzymes (Fig. 4) (49, 50, 67). Fully in line with this concept, the key enzyme of the pathway, siroheme-containing dissimilatory sulfite reductase (DsrAB) from strain HY1 falls into the rDsr group (i.e., oxidative DsrAB used for sulfur oxidation) (*SI Appendix*, Figs. S7 and S10). It is related to rDsrAB sequences from other Alphaproteobacteria (most notably organisms from the order Hyphomicrobiales). Members of the order Hyphomicrobiales, containing closely related rDsrAB—i.e., *Rhodobium orientis* and *Rhodomicrobium vannielii*—have a documented capacity for autotrophic growth on sulfide or thiosulfate (68, 69). A further closely related rDsrAB sequence is that of a metagenome-assembled genome of a canonical sulfur-oxidizing phototroph (purple nonsulfur bacterium) of the genus *Rhodomicrobium*, recovered from a permafrost thaw wetland, which was also found to contain sMMO and PMO gene clusters (26).

The protein DsrC (MHY1_00084) is characterized by a conserved carboxyl-terminal motif ($Cys_B–X_{10}–Cys_A$) and plays a central role in the rDsr pathway, as it acts as a sulfur carrier that is loaded by DsrEFH (70). The membrane-bound DsrMKJOP complex is assumed to oxidize persulfurated DsrC, thus generating DsrC trisulfide, which then serves as the substrate for rDsrAB. The electrons released by the oxidation of the sulfur bridged between DsrC-Cys_A and Cys_B to sulfite are probably transferred to NAD^+. This reaction is catalyzed by the NADH:acceptor oxidoreductase DsrL (MHY1_00087) (49, 71, 72). Notably, two additional DsrC-like proteins are encoded in strain HY1 (MHY1_00075 and MHY1_00097). Both lack Cys_A and probably function as regulatory sulfur-related proteins (RpsA) (73).

In strain HY1, sulfite formed by the rDsr pathway does not appear to be further processed in the cytoplasm, as genes encoding adenosine-5′-phosphosulfate reductase (AprBA) and ATP sulfurylase (Sat) (49) or the cytoplasmically oriented membrane-bound sulfite-oxidizing enzyme SoeABC (74) are all absent. Instead, sulfite is probably transported to the periplasm

by a TauE-like exporter (MHY1_01299) (75) and oxidized to sulfate by periplasmic sulfite:cytochrome *c* oxidoreductase (SorAB; MHY1_p00095–96 residing on the megaplasmid in strain HY1).

Within the family Beijerinckiaceae, genetic equipment of sulfur oxidation closely resembling that of strain HY1 is found in *Rhodoblastus acidophilus* (Fig. 1 and *SI Appendix*, Figs. S7 and S10), but, surprisingly, the growth of this bacterium was not supported by sulfur compounds in laboratory tests (76).

A putative cytoplasmic αβγδ-heterotetrameric, bidirectional hydrogenase is also encoded by MHY1_02662–2665. This resembles *Pyrococcus furiosus* sulfhydrogenase that catalyzes H_2 production and H_2 oxidation coupled with the reduction of elemental sulfur and polysulfide to sulfide (77, 78). The importance of this enzyme for sulfur metabolism is unclear.

Genes Encoding Autotrophy. In order for strain HY1 to grow by oxidizing reduced sulfur as electron donors, a system for autotrophic CO_2 fixation is required since the serine cycle can be used only in conjunction with methane or methanol oxidation. Indeed, strain HY1 encodes genes required for a complete Calvin–Benson–Bassham (CBB) cycle, as observed in other methylotrophs and methanotrophs of the family Beijerinckiaceae (Fig. 1 and Dataset S2). The RubisCO large subunit (CbbL) of strain HY1 shares 94.5 to 96.1% amino acid similarities with the form I enzyme from strains of *Methylocella* and *Methylocapsa*. The CBB cycle is widespread in proteobacterial autotrophic sulfur oxidizers (51) and is also used for chemolithotrophic and methanotrophic growth by verrucomicrobial methanotrophs (20, 79). A methylotroph closely related to HY1, *Beijerinckia mobilis*, also grows autotrophically on methanol by using the CBB cycle (80), further suggesting the possible role of this cycle in carbon fixation during the growth of strain HY1 on sulfur compounds. In contrast, none of the gammaproteobacterial methanotrophs with the complete Sox system contained *cbbL* and *cbbS* genes for the CBB cycle (Fig. 1), which may explain the inability of gammaproteobacterial methanotrophs to grow chemolithoautotrophically.

As expected, the growth of strain HY1 at pH 4.5 with methane, thiosulfate, or both as substrates was strictly dependent on CO_2 supplementation in the headspace (10%, vol/vol), possibly due to the requirement for CO_2 fixation via the serine or CBB cycle (*SI Appendix*, Fig. S11). Similarly, the growth of verrucomicrobial methanotrophs requires supplementation of the medium with CO_2 (19, 20). This indicates that a high mixing ratio of CO_2 is critical for autotrophs growing at acidic pH below the pK_a of bicarbonate (pH 6.1), at which bicarbonate is converted to CO_2, which has limited water solubility.

Induction of Methane and Sulfur Oxidation. To determine whether methane and sulfur metabolisms are constitutive or inducible in strain HY1, oxygen-consumption rates were measured in microrespirometry experiments by using whole cells grown on methane, thiosulfate, or methane+thiosulfate (Table 2). Methane-grown cells consumed oxygen in the presence of methane, but not in the presence of reduced sulfur compounds. Similarly, thiosulfate-grown cells could not consume oxygen in the presence of methane. Thus, neither methanotrophy nor oxidative sulfur metabolism is constitutive. Thiosulfate-grown cells actively consumed oxygen in the presence of tetrathionate, indicating that the S_4I pathway is involved in thiosulfate oxidation. Both methane- and thiosulfate-grown cells consumed oxygen with methanol, ethanol, and 1-propanol at similar rates, indicating constitutive expression of alcohol-utilization enzymes (Table 2).

Oxygen-consumption rates of thiosulfate-grown cells on reduced sulfur compounds (except for elemental sulfur) were 1.8 to 2.7 times higher than those of methane-grown cells on methane (Table 2), coinciding with the higher μ_{max} on thiosulfate than on methane (Fig. 2). Although the affinity of methane-grown cells for methane [$K_{m(app)}$ = 148 ± 20 μM] was 12 times higher than that of thiosulfate-grown cells for thiosulfate [$K_{m(app)}$ = 1,859 ± 76 μM] (*SI Appendix*, Fig. S12), the affinity of thiosulfate-grown cells to sulfide [$K_{m(app)}$ = 2.7 ± 0.2 μM] was much higher. Sulfide is a common and preferred sulfur species by all sulfur-oxidizing lithotrophs (71, 81). The affinity of the methane-grown cells to methane is similar to values estimated in other methanotrophs containing sMMO, but much lower than the affinities estimated in methanotrophs containing pMMO (12, 82, 83). Since methane concentrations in Yongneup (*Materials and Methods*) are less than the $K_{m(app)}$, the low-affinity sMMO-methanotroph strain HY1 may benefit greatly from utilizing other energy sources, such as substrates containing carbon–carbon bonds and reduced sulfur compounds (Table 1).

In the thiosulfate+methane batch cultures, methane and thiosulfate were oxidized concomitantly for growth (*SI Appendix*, Fig. S4). As expected, both methane and thiosulfate contributed

Table 2. Substrate-specific oxygen-consumption rate by strain HY1

	Oxygen uptake rate (μmol·mg·protein^{-1}·h^{-1})		
Substrate	Methane-grown cells	Thiosulfate-grown cells	Methane+thiosulfate-grown cells
Tetrathionate	nd	9.36 ± 0.53	1.53 ± 0.07
Thiosulfate	nd	7.97 ± 0.41	1.40 ± 0.05
Sulfur	nd	2.22 ± 0.11	0.28 ± 0.01
Sulfite	0.51 ± 0.02*	6.34 ± 0.38	1.01 ± 0.05
Sulfide	nd	6.53 ± 0.27	1.21 ± 0.04
Methane	3.48 ± 0.18	nd	2.20 ± 0.11
Methanol	7.64 ± 0.39	4.95 ± 0.21	6.54 ± 0.33
Ethanol	5.45 ± 0.24	4.59 ± 0.26	5.10 ± 0.32
1-Propanol	5.15 ± 0.29	4.11 ± 0.19	4.75 ± 0.22
2-Propanol	nd	nd	nd
Methane+thiosulfate	nt	nt	2.52 ± 0.14

Data are expressed as means ±1 SD (n = 5). Values (μmol·mg·protein^{-1}·h^{-1}) are calculated based on the amount of substrate consumed by resting cell suspension at OD_{600} = 0.3. The substrates' concentrations tested were as follows: 500 μM methane; 20 μM alcohol, sulfite, and sulfide; 4 mM thiosulfate and tetrathionate; and 100 mg of sulfur in a 1-mL vial. nd, not detected; nt, not tested.
*Reaction stopped in the presence of 200 μM sulfite.

to net O_2 consumption in microrespirometry experiments using cells grown mixotrophically on methane and thiosulfate (Table 2). These results support that methane- and thiosulfate-oxidation pathways functioned concurrently during the oxidation of both methane and thiosulfate (*SI Appendix*, Fig. S13*A*). Accordingly, genes of the serine and CBB cycles for CO_2 fixation were expressed during simultaneous oxidation of methane and thiosulfate (*SI Appendix*, Fig. S13*B*). In the microrespirometry experiments, substrate-specific oxygen-consumption rates for each substrate in the mixotrophically grown cells were lower than those in cells grown on either substrate alone. Consistent with this, the mixotrophic growth rate (μ_{max} = 0.023 ± 0.001 h^{-1}) (*SI Appendix*, Fig. S4) was also lower than the growth rate on thiosulfate (μ_{max} = 0.033 ± 0.004 h^{-1}), although similar to the growth rate on methane (μ_{max} = 0.022 ± 0.006 h^{-1}) (Fig. 2). The facultative methanotroph *Methylocystis* sp. H2s was also shown to grow more slowly in the presence of methane and acetate than when methane was provided as the only available substrate (13). As demonstrated in other microorganisms (13, 84, 85), our results indicate that simultaneous utilization of methane and sulfur compounds by strain HY1 may not result in higher growth rates than when a single substrate is utilized, although they do benefit from a greater total substrate pool (Fig. 3).

Carbon Monoxide and Hydrogen Metabolism. Strain HY1 possesses *coxLMS*, encoding carbon monoxide dehydrogenase (CODH) (Dataset S2), which is rare in methanotrophs and found only in the genomes of *Methyloferula stellata* and *M. gorgona* (16, 17, 86). The CODH belongs to the form I type, which can be used for the respiratory oxidation of CO (87) (*SI Appendix*, Fig. S14). Although strain HY1 could not grow with CO as the sole energy source, CO (<5% CO, vol/vol, in headspace) was concomitantly consumed in the presence of other electron donors, such as methane or thiosulfate (*SI Appendix*, Fig. S15). Similarly, *M. gorgona* was found to oxidize CO only in the presence of methane (18). The inability to grow on CO as a sole substrate is unexpected since strain HY1 contains a complete CBB cycle to support CO_2 fixation. The inability of *M. silvestris* $BL2^T$ to grow on methane in the presence of CO suggests a function of CODH for detoxification of CO (*SI Appendix*, Fig. S16). Other potential advantages of CO oxidation in strain HY1, such as increasing starvation survival (86), are yet unclear.

Although many methanotrophs encode hydrogenases (20), strain HY1 encodes a Group 1e Isp-type hydrogenase, which has not been found in any other methanotroph (*SI Appendix*, Fig. S17). The genes encoding large, small, and membrane-anchored subunits of hydrogenase are located adjacently on the megaplasmid and are closely related to genes in other sulfur-oxidizing bacteria (e.g., 79.1% and 71.2% similarity with large and small subunits of hydrogenase in *Acidithiobacillus sulfuriphilus*, respectively) (Dataset S2). Proteobacterial methanotrophs can consume H_2, although, to date, this process has only been reported as providing reductants to supplement methanotrophic growth (88–90). Strain HY1 could not consume H_2 under any conditions, but a trace amount of hydrogen was accumulated during methane oxidation (*SI Appendix*, Fig. S15). Since this type of hydrogenase is reversible (91, 92), excess reducing power generated from electron donors could be diverted to proton reduction to produce H_2, as observed in other methanotrophs (93–95) and thiotrophs (96, 97).

Proteomic Analyses. In order to provide evidence supporting the predicted pathways of reduced sulfur oxidation and methane oxidation in strain HY1 (Fig. 4), proteomes from cells grown on methane and thiosulfate were compared (see the expression of key and all proteins in Datasets S2 and S3, respectively). The proteome of ethanol-grown cells was analyzed for comparison.

The abundances of the structural (MmoX, MmoY, and MmoZ) and chaperone (MmoG) proteins for sMMO were not significantly different between methane- and thiosulfate-grown cells, falling in the range of 0.5 to 4.1% of the total proteins. Abundances of these proteins were higher than those in ethanol-grown cells (Dataset S2). The high abundance of Mmo proteins in thiosulfate-grown cells was unexpected since these cells did not consume oxygen in the microrespirometry experiments when provided with methane as the sole substrate (Table 2). Expression of some genes encoding MMO in the absence of methane was observed previously (19, 98). The presence of these proteins in all of the conditions tested might be an adaptive regulatory trait for rapid induction of methane oxidation in response to dynamic fluxes of methane in wetland environments. The reductase (MmoC), regulatory proteins (MmoD and MmoB), and transcription factor (MmoR), which are all necessary for sMMO activity, were more than threefold increased ($P < 0.05$) in the methane-grown cells compared with thiosulfate- and ethanol-grown cells, potentially explaining why methane oxidation was observed only in methane-grown cells (Table 2). MDH XoxF5 (MHY1_02202; 3.9 to 7.0% of proteins) and cytochrome c_{553i}, XoxG5 (MHY1_00490; 0.12 to 0.27% of proteins) were constitutively expressed on all growth substrates. Proteins involved in H_4MPT-mediated formaldehyde oxidation to formate, aldehyde oxidation, and propionate metabolism were also constitutively expressed (Dataset S2). These results are consistent with the observed oxygen consumption in the presence of various primary alcohols by cells grown on all the three substrates (Table 2) and might be associated with preferential oxidation of methanol over methane (or thiosulfate), as observed in other methanotrophs possessing only sMMO (11, 17, 99). Among chemotaxis receptor proteins, an aerotaxis receptor (Aer) (MHY1_p00042) was more than 2.6-fold ($P < 0.05$) more abundant in methane-grown cells than in other conditions. The increased abundance of flagellin and structural proteins of flagella formation in the methane-grown cells compared to thiosulfate- and ethanol-grown cells indicates that motility is important during growth on methane to allow cells to locate optimal conditions within steep methane and O_2 gradients.

The abundances of proteins predicted to be involved in sulfur oxidation in strain HY1, such as the Sox and rDsr systems, DoxAD/TetH, SorAB, and sulfhydrogenase, were all greatly increased in thiosulfate-grown cells compared with methane- and ethanol-grown cells (Fig. 4 and Dataset S2). For example, the abundance of key Sox (e.g., SoxYZ) and rDsr (e.g., DsrEFH) proteins was >31-fold ($P < 0.05$) higher in thiosulfate-grown than in methane- or ethanol-grown cells. Selective occurrence of DoxAD/TetH in thiosulfate-grown cells indicates the operation and relevance of the S_4I pathway as expected from the microrespirometry experiments (Table 2). The abundances of two types of cytochromes, a homolog of cytochrome c_2 (MHY1_02786) and the cytochrome c_{552} (CycM; MHY1_01465), increased in thiosulfate-grown cells compared with methane-grown cells (more than threefold, $P < 0.05$), indicating that they may transport electrons from sulfur oxidation to the terminal oxidase. Notably, the subunits of high-affinity cbb_3-type cytochrome *c* oxidase were >2.7-fold more abundant ($P < 0.05$) in thiosulfate-grown cells than in cells grown on other substrates (Dataset S2), although cells were grown under oxygen-replete

conditions (>15%, vol/vol). Sulfur oxidation in strain HY1 might be facilitated in microaerobic oxic–anoxic transition zones. The expression of key enzymes of the CBB cycle (CbbL and CbbS) significantly increased (>4.8-fold, $P < 0.05$) in thiosulfate-grown cells compared to methane-grown or ethanol-grown cells (Dataset S2). This result supports the coupled induction of sulfur oxidation and the CBB cycle during chemolithoautotrophic growth of strain HY1.

An N-type ATPase-encoding operon was found in addition to the other F-type ATPase-encoding operons in strain HY1 (Dataset S2). Biochemical evidence indicates that the c-subunits of *Burkholderia pseudomallei* N-type ATPase predominantly bind H^+ and are involved in pumping protons (100). Thr65, Met66, and Tyr69 in the C-terminal helix, which are likely to contribute to the hydrogen-bonding network around the proton-binding site, were conserved in the c-subunit sequence of strain HY1 N-type ATPase (*SI Appendix*, Fig. S18). In addition, we speculate that the N-type ATPase of strain HY1 may function as an ATP-driven proton pump for H^+ homeostasis to survive in acidic stress caused by sulfur oxidation, as observed previously (100). In support of this notion, the N-type ATPase operon is selectively expressed in the cells grown on thiosulfate compared to methane (Dataset S2).

Ecological Relevance. Wetlands are periodically or permanently water-saturated soil environments with a water table at or close to the soil surface. Consequently, steep gradients in soil-redox conditions are developed by a complex pattern of biogeochemical cycling of elements. While the environmental activity of strain HY1 remains unknown, its ability for complete sulfur oxidation could be critical for replenishing the sulfate pool and sustaining sulfate reduction in wetlands. When methane production is repressed by the presence of an active sulfur-redox cycle, thiotrophic capacity could greatly benefit methanotrophs that harbor only sMMO, an enzyme with a low methane affinity (*SI Appendix*, Fig. S12), by allowing them to switch between methane and sulfur oxidation, depending on which substrate is more available (12, 83).

Due to the changes in groundwater tables, wetlands frequently shift in the dominance of sulfate reduction over methanogenesis and vice versa (101, 102). As shown in Table 2, activities of mixotrophically grown cells of strain HY1 to sulfur species and methane were lower than those of thiosulfate- or methane-grown cells of strain HY1. Concordantly, the growth rate of strain HY1 simultaneously utilizing methane and thiosulfate was not higher than those utilizing thiosulfate or methane as a single substrate (Fig. 2 and *SI Appendix*, Fig. S4). This growth pattern is well-described in microorganisms simultaneously utilizing multiple substrates (13, 84). In this context, metabolically flexible thiotrophic methanotrophs may outcompete strict methanotrophs or thiotrophs only in highly fluctuating environments, where they have access to a greater pool of net substrates.

Conclusions

A methanotrophic bacterium showing respiratory oxidation of sulfur compounds was discovered, which greatly expands the current concept of facultative methanotrophy. This study revealed that thiotrophy and methanotrophy are metabolically compatible, which blurs the long-observed distinctness of methanotrophic and thiotrophic microorganisms. It also highlights the difficulties in inferring methanotrophy and thiotrophy based on phylogeny. Further studies on the regulation, kinetics, and evolution of thiotrophic and methanotrophic metabolisms in this strain are required. Due to possible combination with other metabolisms, unexpected metabolic versatility of methanotrophs could remain to be discovered in various sediment environments. Together, our findings set a framework for better understanding methane- and sulfur-cycle interaction in the oxic–anoxic interface zone of natural and engineered ecosystems.

Isolated *Methylovirgula* Species. Strain HY1 is a novel species of the genus *Methylovirgula* of the family Beijerinckiaceae and is capable of both methane and sulfur oxidation for growth. We propose the following candidate status:

Taxonomy.

(i) Etymology. The taxonomy for *Methylovirgula thiovorans* sp. nov. is as follows: thi.o.vo'rans. Gr. neut. n. theion, sulfur; L. pres. part. vorans, eating; N.L. part. adj. thiovorans, sulfur-eating.

(ii) Habitat. An acidic wetland on top of Mount (Mt.) Daeam located in South Korea.

(iii) Diagnosis. Cells are straight rods, with a diameter of 0.2 to 0.3 μm and a length of 0.4 to 1.7 μm (*SI Appendix*, Fig. S19). Grows between 15 and 30 °C with an optimum at 27 °C and between pH 4.0 to 6.0 with an optimum at pH 4.5. The strain grows via oxidizing methane, various multicarbon organic compounds, and reduced sulfur compounds (Table 1). The G + C content of the type strain is 60.1 mol%. The 16S rRNA gene sequence similarity is 98.7% with *M. ligni* and ranges from 95.8 to 97.3% with closely related genera: *Methylocapsa*, *Methyloferula*, *Beijerinckia*, and *Methylocella*.

Materials and Methods

Sampling, Enrichment, and Isolation. Peat samples were collected in August 2016 from Yongneup (38°12′53.6″ N, 128°07′27.3″ E), an acidic wetland (pH 4.2 to 6.4) located at the northwestern slope of Mt. Daeam (1,200 to 1,280 m above sea level), Korea. The samples were taken from a depth of 0 to 5 cm below the peat-bog surface for cultivation. The average temperature was 10.0 °C, and the annual precipitation was 1,187.5 mm. In the 30-cm column obtained in November 2021, sulfate and methane concentrations were 8.6 to 38.9 μM and 1.2 to 41.3 μM, respectively. Sulfide and elemental sulfur concentrations were below the detection level. The conductivity of pore water was in the range of 15.2 to 34.7 μS/cm. The oxygen penetration depth into the wetland was less than 1 mm. Analytical methods are described in *SI Appendix, Analytical Methods*. After transporting the samples to the laboratory, they were stored at 4 °C before use, and 5 g of sample was immediately frozen for 16S rRNA gene-amplicon sequencing (see below). Enrichment of methanotrophs is described in *SI Appendix, Enrichment*. Pure cultures of the methane-oxidizers were obtained by repeatedly diluting the enrichment cultures as described (103). The most diluted culture showing methane oxidation was serially diluted and filtered through 0.2-μm Track-Etch membrane polycarbonate filters (Whatman). The filters were placed on LSM medium in Petri dishes and incubated in airtight containers containing CH_4 (20%, vol/vol) and CO_2 (5%, vol/vol) in air at 25 °C. Colonies that appeared after 3 wk of incubation were transferred to fresh LSM medium in serum vials with the same gas composition. Individual isolates were identified by sequencing the 16S rRNA gene with the 27F/1492R (104) primer set. Isolation in axenic culture was confirmed by seeding aliquots of the methane-grown cultures into LSM medium with 0.05% (weight/vol) yeast extract, tryptic soy broth, and Luria–Bertani broth without CH_4 and incubated at 25 °C. No growth was observed in these media. To confirm the purity of the isolated strain from methane-grown culture, 16S rRNA gene-amplicon sequencing was performed and confirmed the presence of a single strain (*SI Appendix, 16S rRNA Gene Amplicon Library Analysis*). The isolated methanotrophic strain was routinely maintained on solid and liquid LSM with methane as an energy source.

Batch-Culture Growth Experiments. Unless stated otherwise, growth experiments were performed in 160-mL serum bottles containing 20 mL of LSM medium and inoculated with 1 to 10% (vol/vol) actively growing cells from the

log phase (starting optical density values at 600 nm [OD_{600}] < 0.08) with the appropriate carbon and energy sources of interest. To avoid the carryover of other substrates during inoculation, cells grown over multiple transfers on the substrate of interest or washed cells grown on a different substrate were used as inoculum. For washing, cells were centrifuged at 4,000 × *g* for 20 min and washed twice with fresh basal LSM medium. The culture incubations were performed at 25 °C with shaking at 200 rpm. Growth of the strain was determined by monitoring changes in OD_{600} of the culture using a spectrophotometer (Optizen 2120UV, Mecasys Co.) and real-time quantification of 16S rRNA gene abundances using the 518F/786R primer set (105). The specific growth rate was calculated by determining the slope of the Log_{10}-transformed OD_{600} values plotted against time. Specific analytical methods for the determination of CH_4, CO_2, CO, H_2, sulfate, thiosulfate, cellular protein concentration, and dry cell weight in batch cultures are all described in *SI Appendix, Analytical Methods*. Determination of the optimal pH and temperature, utilization of different growth substrates, carbon dioxide requirement, and dependency on lanthanide were performed as described in *SI Appendix, Growth Properties*.

DNA Isolation, Genome Analysis, and Phylogenetic Analysis. Extraction of high-molecular-weight genomic DNA from strain HY1 and genome sequencing is described in *SI Appendix, Genomic and Phylogenetic Analyses*. Annotation of the assembled genome was performed with the Prokka annotation pipeline (version [v]1.14.6) (106), MicroScope (107), and PATRIC (108) annotation platforms. Functional assignment of the predicted genes was improved by using a set of public databases [InterPro (109), Gene Ontology (110, 111), Pfam (112), the Conserved Domains Database (113), TIGRFAM (114), and EggNOG (115)]. Prediction of signal peptides and transmembrane helices was performed by using the web-based services SignalP (v5.0) (116) and TMHMM (v2.0) (117) with default settings. For calculation of average nucleotide identity value of strain HY1 compared to reference genomes, the Orthologous Average Identity Tool was used (118). Phylogenomic analysis of strain HY1 was performed by following the Anvi'o phylogenomics workflow (119), described in detail in *SI Appendix, Genomic and Phylogenetic Analyses*. Phylogenetic analyses of the 16S rRNA gene, methane monooxygenase (MmoXYBZDC), large subunits of the carbon monoxide dehydrogenase (CoxL), [NiFe]-hydrogenases (HydB), DsrAB, and SoxB of strain HY1 are described in *SI Appendix, Genomic and Phylogenetic Analyses*.

Microrespirometry and Kinetics Experiments. Substrate-dependent oxygen consumption of methane-, thiosulfate-, or methane+thiosulfate-grown cells was assayed in a 2-mL microrespiration chamber, as detailed in *SI Appendix, Assay of Oxygen Consumption*. To avoid the carryover of alternate substrates, cells were grown over multiple transfers on a substrate of interest and washed twice in basal LSM medium before inoculation into the microrespiration chamber. To calculate substrate oxidation rate based on the measured oxygen-consumption rate, the stoichiometry of substrate respiration (substrate vs. O_2) was obtained from microrespirometry experiments. The stoichiometries of methane, thiosulfate, and sulfide oxidation to oxygen consumption were estimated as 1:1.57, 1:1.65, and 1:1.64, respectively, and were in a similar range with those of microorganisms with the same metabolic pathways (120, 121). The Michaelis–Menten equation (Eq. **2**) was fitted to the O_2 and substrate oxidation rates to estimate the kinetics constants, $K_{m(app)}$ and V_{max}, while the specific affinity (a^o) was estimated from the $K_{m(app)}$ and V_{max} values (Eq. **3**) as described (122).

$$v = (V_{max} \times [S]) \times \left(K_{m(app)}\right) + [S])^{-1}, \quad [2]$$

$$a^o = V_{max} \times {K_{m(app)}}^{-1}, \quad [3]$$

where v represents the oxidation rate (expressed in $\mu M \cdot h^{-1}$) and V_{max} denotes the maximum rate (expressed in $\mu M \cdot h^{-1}$). For comparison and calculation of a^o, the V_{max} is divided by cellular protein concentration ($mg \cdot protein \cdot L^{-1}$) and expressed in $\mu mol \cdot mg \cdot protein^{-1} \cdot h^{-1}$. $K_{m(app)}$ is the apparent Michaelis–Menten half-saturation constant (in μM), [S] represents the substrate concentration (μM), and a^o is the specific affinity ($L \cdot mg \cdot protein^{-1} \cdot h^{-1}$).

Transcriptome and Proteome Analyses. To avoid the carryover of substrates, cells grown over multiple transfers on a substrate of interest were used for transcriptomic and proteomic analyses. For analysis of expression of genes of CO_2 fixation pathways, transcriptome analysis was performed as described in detail in *SI Appendix, Transcriptome Analysis*. For proteome analysis, cells of strain HY1 were cultivated in 160-mL serum vials containing 20 mL of medium at pH 5.0 with headspace containing CO_2 (10%, vol/vol). Methane (20%, vol/vol), thiosulfate (8 mM), or ethanol (20 mM) was used individually as a sole energy source. A set of four replicates were conducted for each growth condition. The cells were harvested at the midexponential phase (methane and ethanol, $OD_{600} = 0.2$; thiosulfate, $OD_{600} = 0.1$) at 5,000 × *g* (10 min, 25 °C). The cell pellets were frozen immediately in liquid dinitrogen and stored at −80 °C until analyses. Mass spectrometric analysis of peptide lysates, raw data processing, and statistical analysis are described in detail in *SI Appendix, Proteome Analysis*.

Data Availability. The complete genome sequence of strain HY1 was deposited in the National Center for Biotechnology Information (NCBI) GenBank (accession nos. CP073764 (128) [Chromosome] and CP073765 (129) [Megaplasmid]). The mass spectrometry proteomics data have been deposited to the ProteomeXchange Consortium via the Proteomics Identification Database (123) partner repository with (dataset identifier PXD025979) (130). The whole-transcriptome data were deposited in the NCBI BioProject database (accession no. PRJNA790002) (131).

ACKNOWLEDGMENTS. This work was supported by the Basic Science Research Program through the National Research Foundation of Korea (NRF) funded by the Korean government (Ministry of Education) (2020R1A6A1A06046235); NRF grants funded by the Korean government (Ministry of Science and ICT) (2021R1A2C3004015); and the National Institute of Agricultural Science, Ministry of Rural Development Administration, Republic of Korea (PJ01700703). We are grateful to the contribution of Dr. So-Jeong Kim of the Korea Institute of Geoscience and Mineral Resources, Daejeon; and Drs. Sung Gyun Kang and Hae Chang Jung of the Korea Institute of Ocean Science and Technology, Busan, toward gas analysis. We thank Dr. Myung-Suk Kang of the National Institute of Biosciences and Bioresources, Korea, for access to the sampling sites. A.L. was supported by the Austrian Science Fund (FWF Project P 31996-B); P.F.D. was supported by a Natural Sciences and Engineering Research Council of Canada Discovery Grant (NSERC-RGPIN-2019-06265); and K.D.K. was supported by the European Union (MSCA-IF project 796687–H2Gut).

Author affiliations: [a]Department of Biological Sciences and Biotechnology, Chungbuk National University, Seowon-Gu, Cheongju 28644, Republic of Korea; [b]Department of Molecular Systems Biology, Helmholtz Centre for Environmental Research–Zentrum für Umweltforschung GmbH, 04318 Leipzig, Germany; [c]Institute of Biochemistry, Faculty of Biosciences, Pharmacy and Psychology, University of Leipzig, 04103 Leipzig, Germany; [d]Division of Microbial Ecology, Centre for Microbiology and Environmental Systems Science, University of Vienna, Vienna, 1030; Austria; [e]Department of Biological Sciences, University of Calgary, Calgary, AB T2N 1N4, Canada; [f]Institute for Microbiology and Biotechnology, Rheinische Friedrich-Wilhelms-Universität Bonn, 53115 Bonn, Germany; and [g]Department of Marine Science and Convergence Engineering, Hanyang University, Ansan 15588, Republic of Korea

1. G. Allen, Biogeochemistry: Rebalancing the global methane budget. *Nature* **538**, 46–48 (2016).
2. M. Saunois, R. B. Jackson, P. Bousquet, B. Poulter, J. G. Canadell, The growing role of methane in anthropogenic climate change. *Environ. Res. Lett.* **11**, 120207 (2016).
3. E. Matthews, "Wetlands" in *Atmospheric Methane: Its Role in the Global Environment* , M. A. K. Khalil, Ed. (Springer Berlin Heidelberg, Berlin, 2000), pp. 202–233.
4. J. T. Houghton *et al.*, *Climate Change 2001: The Scientific Basis: Contribution of Working Group I to the Third Assessment Report of the Intergovernmental Panel on Climate Change* (Cambridge University Press, Cambridge, UK, 2001).
5. R. Conrad, F. Rothfuss, Methane oxidation in the soil surface layer of a flooded rice field and the effect of ammonium. *Biol. Fertil. Soils* **12**, 28–32 (1991).
6. J. B. Yavitt, G. E. Lang, D. M. Downey, Potential methane production and methane oxidation rates in peatland ecosystems of the Appalachian Mountains, United States. *Global Biogeochem. Cycles* **2**, 253–268 (1988).
7. H. Zhang *et al.*, Methane production and oxidation potentials along a fen-bog gradient from southern boreal to subarctic peatlands in Finland. *Glob. Change Biol.* **27**, 4449–4464 (2021).
8. H. J. Laanbroek, Methane emission from natural wetlands: Interplay between emergent macrophytes and soil microbial processes. A mini-review. *Ann. Bot.* **105**, 141–153 (2010).
9. F. N. Ponnamperuma, "The chemistry of submerged soils" in *Advances in Agronomy*, N. C. Brady, Ed. (Academic Press, New York, 1972), vol. **24**, pp. 29–96.

10. G. Muyzer, A. J. M. Stams, The ecology and biotechnology of sulphate-reducing bacteria. *Nat. Rev. Microbiol.* **6**, 441–454 (2008).
11. S. N. Dedysh, C. Knief, P. F. Dunfield, *Methylocella* species are facultatively methanotrophic. *J. Bacteriol.* **187**, 4665–4670 (2005).
12. A. T. Crombie, J. C. Murrell, Trace-gas metabolic versatility of the facultative methanotroph *Methylocella silvestris. Nature* **510**, 148–151 (2014).
13. S. E. Belova *et al.*, Acetate utilization as a survival strategy of peat-inhabiting *Methylocystis* spp. *Environ. Microbiol. Rep.* **3**, 36–46 (2011).
14. J. Im, S.-W. Lee, S. Yoon, A. A. Dispirito, J. D. Semrau, Characterization of a novel facultative *Methylocystis* species capable of growth on methane, acetate and ethanol. *Environ. Microbiol. Rep.* **3**, 174–181 (2011).
15. P. F. Dunfield, S. E. Belova, A. V. Vorob'ev, S. L. Cornish, S. N. Dedysh, *Methylocapsa aurea* sp. nov., a facultative methanotroph possessing a particulate methane monooxygenase, and emended description of the genus *Methylocapsa. Int. J. Syst. Evol. Microbiol.* **60**, 2659–2664 (2010).
16. A. T. Tveit *et al.*, Widespread soil bacterium that oxidizes atmospheric methane. *Proc. Natl. Acad. Sci. U.S.A.* **116**, 8515–8524 (2019).
17. A. V. Vorobev *et al.*, *Methyloferula stellata* gen. nov., sp. nov., an acidophilic, obligately methanotrophic bacterium that possesses only a soluble methane monooxygenase. *Int. J. Syst. Evol. Microbiol.* **61**, 2456–2463 (2011).
18. A. T. Tveit *et al.*, Simultaneous oxidation of atmospheric methane, carbon monoxide and hydrogen for bacterial growth. *Microorganisms* **9**, 153 (2021).
19. S. Mohammadi, A. Pol, T. A. van Alen, M. S. M. Jetten, H. J. M. Op den Camp, *Methylacidiphilum fumariolicum* SolV, a thermoacidophilic 'Knallgas' methanotroph with both an oxygen-sensitive and -insensitive hydrogenase. *ISME J.* **11**, 945–958 (2017).
20. C. R. Carere *et al.*, Mixotrophy drives niche expansion of verrucomicrobial methanotrophs. *ISME J.* **11**, 2599–2610 (2017).
21. S. S. Mohammadi *et al.*, The acidophilic methanotroph *Methylacidimicrobium tartarophylax* 4AC grows as autotroph on H_2 under microoxic conditions. *Front. Microbiol.* **10**, 2352 (2019).
22. N. Picone *et al.*, *Methylacidimicrobium thermophilum* AP8, a novel methane- and hydrogen-oxidizing bacterium isolated from volcanic soil on Pantelleria Island, Italy. *Front. Microbiol.* **12**, 637762 (2021).
23. R. A. Schmitz *et al.*, Verrucomicrobial methanotrophs: Ecophysiology of metabolically versatile acidophiles. *FEMS Microbiol. Rev.* **45**, fuab007 (2021).
24. S. I. Awala *et al.*, Verrucomicrobial methanotrophs grow on diverse C3 compounds and use a homolog of particulate methane monooxygenase to oxidize acetone. *ISME J.* **15**, 3636–3647 (2021).
25. R. A. Schmitz *et al.*, Methanethiol consumption and hydrogen sulfide production by the thermoacidophilic methanotroph *Methylacidiphilum fumariolicum* SolV. *Front. Microbiol.* **13**, 857442 (2022).
26. C. M. Singleton *et al.*, Methanotrophy across a natural permafrost thaw environment. *ISME J.* **12**, 2544–2558 (2018).
27. S. N. Dedysh, "Methylovirgula" in *Bergey's Manual of Systematics of Archaea and Bacteria*, S. D. M. E. Trujillo *et al.*, Eds. (Wiley, Hoboken, NJ, 2016), pp. 1–5.
28. S. N. Dedysh, P. F. Dunfield, "Beijerinckiaceae" in *Bergey's Manual of Systematics of Archaea and Bacteria*, S. D. M. E. Trujillo *et al.*, Eds. (Wiley, Hoboken, NJ, 2016), pp. 1–4.
29. M. Farhan Ul Haque, H. J. Xu, J. C. Murrell, A. Crombie, Facultative methanotrophs–diversity, genetics, molecular ecology and biotechnological potential: A mini-review. *Microbiology (Reading)* **166**, 894–908 (2020).
30. M. Farhan Ul Haque, A. T. Crombie, J. C. Murrell, Novel facultative *Methylocella* strains are active methane consumers at terrestrial natural gas seeps. *Microbiome* **7**, 134 (2019).
31. J. G. Leahy, P. J. Batchelor, S. M. Morcomb, Evolution of the soluble diiron monooxygenases. *FEMS Microbiol. Rev.* **27**, 449–479 (2003).
32. S. N. Dedysh *et al.*, Draft genome sequence of *Methyloferula stellata* AR4, an obligate methanotroph possessing only a soluble methane monooxygenase. *Genome Announc.* **3**, e01555–e01514 (2015).
33. I. Tamas, A. V. Smirnova, Z. He, P. F. Dunfield, The (d)evolution of methanotrophy in the *Beijerinckiaceae*–a comparative genomics analysis. *ISME J.* **8**, 369–382 (2014).
34. J. T. Keltjens, A. Pol, J. Reimann, H. J. M. Op den Camp, PQQ-dependent methanol dehydrogenases: Rare-earth elements make a difference. *Appl. Microbiol. Biotechnol.* **98**, 6163–6183 (2014).
35. H. J. Op den Camp *et al.*, Environmental, genomic and taxonomic perspectives on methanotrophic *Verrucomicrobia. Environ. Microbiol. Rep.* **1**, 293–306 (2009).
36. M. C. F. van Teeseling *et al.*, Expanding the verrucomicrobial methanotrophic world: Description of three novel species of *Methylacidimicrobium* gen. nov. *Appl. Environ. Microbiol.* **80**, 6782–6791 (2014).
37. A. Pol *et al.*, Rare earth metals are essential for methanotrophic life in volcanic mudpots. *Environ. Microbiol.* **16**, 255–264 (2014).
38. Y. Chen *et al.*, Complete genome sequence of the aerobic facultative methanotroph *Methylocella silvestris* BL2. *J. Bacteriol.* **192**, 3840–3841 (2010).
39. K. E. Martin, J. Ozsvar, N. V. Coleman, SmoXYB1C1Z of *Mycobacterium* sp. strain NBB4: A soluble methane monooxygenase (sMMO)-like enzyme, active on C2 to C4 alkanes and alkenes. *Appl. Environ. Microbiol.* **80**, 5801–5806 (2014).
40. P. R. Tupa, H. Masuda, Comparative proteomic analysis of propane metabolism in *Mycobacterium* sp. strain ENV421 and *Rhodococcus* sp. strain ENV425. *J. Mol. Microbiol. Biotechnol.* **28**, 107–115 (2018).
41. N. M. Good *et al.*, Pyrroloquinoline quinone ethanol dehydrogenase in *Methylobacterium extorquens* AM1 extends lanthanide-dependent metabolism to multicarbon substrates. *J. Bacteriol.* **198**, 3109–3118 (2016).
42. J. Huang, Z. Yu, L. Chistoserdova, Lanthanide-dependent methanol dehydrogenases of XoxF4 and XoxF5 clades are differentially distributed among methylotrophic bacteria and they reveal different biochemical properties. *Front. Microbiol.* **9**, 1366 (2018).
43. S. Bordel, A. T. Crombie, R. Muñoz, J. C. Murrell, Genome Scale Metabolic Model of the versatile methanotroph *Methylocella silvestris. Microb. Cell Fact.* **19**, 144 (2020).
44. M. K. Sluis *et al.*, Biochemical, molecular, and genetic analyses of the acetone carboxylases from *Xanthobacter autotrophicus* strain Py2 and *Rhodobacter capsulatus* strain B10. *J. Bacteriol.* **184**, 2969–2977 (2002).
45. T. Kotani, H. Yurimoto, N. Kato, Y. Sakai, Novel acetone metabolism in a propane-utilizing bacterium, *Gordonia* sp. strain TY-5. *J. Bacteriol.* **189**, 886–893 (2007).
46. T. Furuya, T. Nakao, K. Kino, Catalytic function of the mycobacterial binuclear iron monooxygenase in acetone metabolism. *FEMS Microbiol. Lett.* **362**, fnv136 (2015).
47. D. R. Koop, J. P. Casazza, Identification of ethanol-inducible P-450 isozyme 3a as the acetone and acetol monooxygenase of rabbit microsomes. *J. Biol. Chem.* **260**, 13607–13612 (1985).
48. S. N. Dedysh, P. F. Dunfield, "Facultative methane oxidizers" in *Taxonomy, Genomics and Ecophysiology of Hydrocarbon-Degrading Microbes* , T. J. McGenity, Ed. (Springer International Publishing, Cham, Switzerland, 2019), pp. 279–297.
49. C. Dahl, Cytoplasmic sulfur trafficking in sulfur-oxidizing prokaryotes. *IUBMB Life* **67**, 268–274 (2015).
50. C. Dahl, "A biochemical view on the biological sulfur cycle" in *Environmental Technologies to Treat Sulfur Pollution. Principles and Engineering*, P. N. L. Lens, Ed. (IWA Publishing, London, ed. 2, 2020), pp. 55–96.
51. N.-U. Frigaard, C. Dahl, "Sulfur metabolism in phototrophic sulfur bacteria" in *Advances in Microbial Physiology*, R. K. Poole, Ed. (Academic Press, New York, 2008), vol. **54**, pp. 103–200.
52. U. Kappler, M. J. Maher, The bacterial SoxAX cytochromes. *Cell. Mol. Life Sci.* **70**, 977–992 (2013).
53. J. M. Kurth *et al.*, Electron accepting units of the diheme cytochrome c TsdA, a bifunctional thiosulfate dehydrogenase/tetrathionate reductase. *J. Biol. Chem.* **291**, 24804–24818 (2016).
54. J. S. Geelhoed, R. Kleerebezem, D. Y. Sorokin, A. J. Stams, M. C. van Loosdrecht, Reduced inorganic sulfur oxidation supports autotrophic and mixotrophic growth of *Magnetospirillum* strain J10 and *Magnetospirillum gryphiswaldense. Environ. Microbiol.* **12**, 1031–1040 (2010).
55. L. Y. Stein *et al.*, Genome sequence of the obligate methanotroph *Methylosinus trichosporium* strain OB3b. *J. Bacteriol.* **192**, 6497–6498 (2010).
56. Z. Bao, R. Shinoda, K. Minamisawa, Draft genome sequence of *Methylosinus* sp. strain 3S-1, an isolate from rice root in a low-nitrogen paddy field. *Genome Announc.* **4**, e00932-16 (2016).
57. A. Saidi-Mehrabad *et al.*, *Methylicorpusculum oleiharenae* gen. nov., sp. nov., an aerobic methanotroph isolated from an oil sands tailings pond. *Int. J. Syst. Evol. Microbiol.* **70**, 2499–2508 (2020).
58. U. Kappler, "Bacterial sulfite-oxidizing enzymes–enzymes for chemolithotrophs only?" in *Microbial Sulfur Metabolism*, C. Dahl, C. G. Friedrich, Eds. (Springer International Publishing, Cham, Switzerland, 2008), pp. 151–169.
59. C. Appia-Ayme, P. J. Little, Y. Matsumoto, A. P. Leech, B. C. Berks, Cytochrome complex essential for photosynthetic oxidation of both thiosulfate and sulfide in *Rhodovulum sulfidophilum. J. Bacteriol.* **183**, 6107–6118 (2001).
60. G. A. De Jong, W. Hazeu, P. Bos, J. G. Kuenen, Isolation of the tetrathionate hydrolase from *Thiobacillus acidophilus. Eur. J. Biochem.* **243**, 678–683 (1997).
61. R. Meulenberg, J. T. Pronk, W. Hazeu, P. Bos, J. G. Kuenen, Oxidation of reduced sulphur compounds by intact cells of *Thiobacillus acidophilus. Arch. Microbiol.* **157**, 161–168 (1992).
62. M. Marcia, U. Ermler, G. Peng, H. Michel, The structure of *Aquifex aeolicus* sulfide:quinone oxidoreductase, a basis to understand sulfide detoxification and respiration. *Proc. Natl. Acad. Sci. U.S.A.* **106**, 9625–9630 (2009).
63. M. Marcia, U. Ermler, G. Peng, H. Michel, A new structure-based classification of sulfide:quinone oxidoreductases. *Proteins* **78**, 1073–1083 (2010).
64. Y. Tanaka *et al.*, Crystal structure of a YeeE/YedE family protein engaged in thiosulfate uptake. *Sci. Adv.* **6**, eaba7637 (2020).
65. T. Koch, C. Dahl, A novel bacterial sulfur oxidation pathway provides a new link between the cycles of organic and inorganic sulfur compounds. *ISME J.* **12**, 2479–2491 (2018).
66. T. Gristwood *et al.*, PigS and PigP regulate prodigiosin biosynthesis in Serratia via differential control of divergent operons, which include predicted transporters of sulfur-containing molecules. *J. Bacteriol.* **193**, 1076–1085 (2011).
67. T. S. Tanabe, S. Leimkühler, C. Dahl, The functional diversity of the prokaryotic sulfur carrier protein TusA. *Adv. Microb. Physiol.* **75**, 233–277 (2019).
68. A. Hiraishi, K. Urata, T. Satoh, A new genus of marine budding phototrophic bacteria, *Rhodobium* gen. nov., which includes *Rhodobium orientis* sp. nov. and *Rhodobium marinum* comb. nov. *Int. J. Syst. Bacteriol.* **45**, 226–234 (1995).
69. J. F. Imhoff, "Rhodomicrobium" in *Bergey's Manual of Systematics of Archaea and Bacteria*, M. E. Trujillo *et al.*, Eds. (John Wiley & Sons, Inc., Hoboken, NJ, 2021), pp. 1–8.
70. Y. Stockdreher *et al.*, Cytoplasmic sulfurtransferases in the purple sulfur bacterium *Allochromatium vinosum*: Evidence for sulfur transfer from DsrEFH to DsrC. *PLoS One* **7**, e40785 (2012).
71. C. Dahl, "Sulfur metabolism in phototrophic bacteria" in *Modern Topics in the Phototrophic Prokaryotes: Metabolism, Bioenergetics, and Omics*, P. C. Hallenbeck, Ed. (Springer International Publishing, Cham, Switzerland, 2017), pp. 27–66.
72. M. Löffler *et al.*, DsrL mediates electron transfer between NADH and rDsrAB in *Allochromatium vinosum. Environ. Microbiol.* **22**, 783–795 (2020).
73. S. S. Venceslau, Y. Stockdreher, C. Dahl, I. A. Pereira, The "bacterial heterodisulfide" DsrC is a key protein in dissimilatory sulfur metabolism. *Biochim. Biophys. Acta* **1837**, 1148–1164 (2014).
74. C. Dahl, B. Franz, D. Hensen, A. Kesselheim, R. Zigann, Sulfite oxidation in the purple sulfur bacterium *Allochromatium vinosum*: Identification of SoeABC as a major player and relevance of SoxYZ in the process. *Microbiology (Reading)* **159**, 2626–2638 (2013).
75. S. Weinitschke, K. Denger, A. M. Cook, T. H. M. Smits, The DUF81 protein TauE in *Cupriavidus necator* H16, a sulfite exporter in the metabolism of C2 sulfonates. *Microbiology (Reading)* **153**, 3055–3060 (2007).
76. J. F. Imhoff, Transfer of *Rhodopseudomonas acidophila* to the new genus *Rhodoblastus* as *Rhodoblastus acidophilus* gen. nov., comb. nov. *Int. J. Syst. Evol. Microbiol.* **51**, 1863–1866 (2001).
77. K. Ma, M. W. Adams, Sulfide dehydrogenase from the hyperthermophilic archaeon *Pyrococcus furiosus*: A new multifunctional enzyme involved in the reduction of elemental sulfur. *J. Bacteriol.* **176**, 6509–6517 (1994).
78. K. Ma, R. Weiss, M. W. Adams, Characterization of hydrogenase II from the hyperthermophilic archaeon *Pyrococcus furiosus* and assessment of its role in sulfur reduction. *J. Bacteriol.* **182**, 1864–1871 (2000).
79. A. F. Khadem *et al.*, Autotrophic methanotrophy in verrucomicrobia: *Methylacidiphilum fumariolicum* SolV uses the Calvin–Benson–Bassham cycle for carbon dioxide fixation. *J. Bacteriol.* **193**, 4438–4446 (2011).

80. S. N. Dedysh *et al.*, Methylotrophic autotrophy in *Beijerinckia mobilis*. *J. Bacteriol.* **187**, 3884–3888 (2005).
81. W. Ghosh, B. Dam, Biochemistry and molecular biology of lithotrophic sulfur oxidation by taxonomically and ecologically diverse bacteria and archaea. *FEMS Microbiol. Rev.* **33**, 999–1043 (2009).
82. C. Knief, P. F. Dunfield, Response and adaptation of different methanotrophic bacteria to low methane mixing ratios. *Environ. Microbiol.* **7**, 1307–1317 (2005).
83. R. Oldenhuis, J. Y. Oedzes, J. J. van der Waarde, D. B. Janssen, Kinetics of chlorinated hydrocarbon degradation by *Methylosinus trichosporium* OB3b and toxicity of trichloroethylene. *Appl. Environ. Microbiol.* **57**, 7–14 (1991).
84. D. Ramkrishna, D. S. Kompala, G. T. Tsao, Are microbes optimal strategists? *Biotechnol. Prog.* **3**, 121–126 (1987).
85. F. Schut *et al.*, Substrate uptake and utilization by a marine ultramicrobacterium. *Microbiology (Reading)* **141**, 351–361 (1995).
86. P. R. F. Cordero *et al.*, Atmospheric carbon monoxide oxidation is a widespread mechanism supporting microbial survival. *ISME J.* **13**, 2868–2881 (2019).
87. G. M. King, C. F. Weber, Distribution, diversity and ecology of aerobic CO-oxidizing bacteria. *Nat. Rev. Microbiol.* **5**, 107–118 (2007).
88. Y. P. Chen, D. C. Yoch, Regulation of two nickel-requiring (inducible and constitutive) hydrogenases and their coupling to nitrogenase in *Methylosinus trichosporium* OB3b. *J. Bacteriol.* **169**, 4778–4783 (1987).
89. N. N. Shah, M. L. Hanna, K. J. Jackson, R. T. Taylor, Batch cultivation of *Methylosinus trichosporium* OB3B: IV. Production of hydrogen-driven soluble or particulate methane monooxygenase activity. *Biotechnol. Bioeng.* **45**, 229–238 (1995).
90. T. Hanczár, R. Csáki, L. Bodrossy, J. C. Murrell, K. L. Kovács, Detection and localization of two hydrogenases in *Methylococcus capsulatus* (Bath) and their potential role in methane metabolism. *Arch. Microbiol.* **177**, 167–172 (2002).
91. C. Greening *et al.*, Genomic and metagenomic surveys of hydrogenase distribution indicate H_2 is a widely utilised energy source for microbial growth and survival. *ISME J.* **10**, 761–777 (2016).
92. L. S. Palágyi-Mészáros *et al.*, Electron-transfer subunits of the NiFe hydrogenases in *Thiocapsa roseopersicina* BBS. *FEBS J.* **276**, 164–174 (2009).
93. A. Gilman *et al.*, Oxygen-limited metabolism in the methanotroph *Methylomicrobium buryatense* 5GB1C. *PeerJ* **5**, e3945 (2017).
94. S. Y. Jo *et al.*, Hydrogen production from methane by *Methylomonas* sp. DH-1 under micro-aerobic conditions. *Biotechnol. Bioprocess Eng. BBE* **25**, 71–77 (2020).
95. M. G. Kalyuzhnaya *et al.*, Highly efficient methane biocatalysis revealed in a methanotrophic bacterium. *Nat. Commun.* **4**, 2785 (2013).
96. R. Tengölics *et al.*, Connection between the membrane electron transport system and Hyn hydrogenase in the purple sulfur bacterium, *Thiocapsa roseopersicina* BBS. *Biochim. Biophys. Acta* **1837**, 1691–1698 (2014).
97. T. V. Laurinavichene, G. Rákhely, K. L. Kovács, A. A. Tsygankov, The effect of sulfur compounds on H_2 evolution/consumption reactions, mediated by various hydrogenases, in the purple sulfur bacterium, *Thiocapsa roseopersicina*. *Arch. Microbiol.* **188**, 403–410 (2007).
98. A. V. Smirnova, P. F. Dunfield, Differential transcriptional activation of genes encoding soluble methane monooxygenase in a facultative versus an obligate methanotroph. *Microorganisms* **6**, 20 (2018).
99. B. Vekeman *et al.*, New *Methyloceanibacter* diversity from North Sea sediments includes methanotroph containing solely the soluble methane monooxygenase. *Environ. Microbiol.* **18**, 4523–4536 (2016).
100. S. Schulz, M. Wilkes, D. J. Mills, W. Kühlbrandt, T. Meier, Molecular architecture of the N-type ATPase rotor ring from *Burkholderia pseudomallei*. *EMBO Rep.* **18**, 526–535 (2017).
101. D. B. Nedwell, A. Watson, CH_4 production, oxidation and emission in a U.K. ombrotrophic peat bog: Influence of SO_4^{2-} from acid rain. *Soil Biol. Biochem.* **27**, 893–903 (1995).
102. A. Watson, D. B. Nedwell, Methane production and emission from peat: The influence of anions (sulphate, nitrate) from acid rain. *Atmos. Environ.* **32**, 3239–3245 (1998).
103. S. I. Awala *et al.*, *Methylococcus geothermalis* sp. nov., a methanotroph isolated from a geothermal field in the Republic of Korea. *Int. J. Syst. Evol. Microbiol.* **70**, 5520–5530 (2020).
104. W. G. Weisburg, S. M. Barns, D. A. Pelletier, D. J. Lane, 16S ribosomal DNA amplification for phylogenetic study. *J. Bacteriol.* **173**, 697–703 (1991).
105. G. Muyzer, E. C. de Waal, A. G. Uitterlinden, Profiling of complex microbial populations by denaturing gradient gel electrophoresis analysis of polymerase chain reaction-amplified genes coding for 16S rRNA. *Appl. Environ. Microbiol.* **59**, 695–700 (1993).
106. T. Seemann, Prokka: Rapid prokaryotic genome annotation. *Bioinformatics* **30**, 2068–2069 (2014).
107. D. Vallenet *et al.*, MicroScope: A platform for microbial genome annotation and comparative genomics. *Database (Oxford)* **2009**, bap021 (2009).
108. J. J. Davis *et al.*, The PATRIC Bioinformatics Resource Center: Expanding data and analysis capabilities. *Nucleic Acids Res.* **48**, D606–D612 (2020).
109. S. Hunter *et al.*, InterPro: The integrative protein signature database. *Nucleic Acids Res.* **37**, D211–D215 (2009).
110. M. Ashburner *et al.*; The Gene Ontology Consortium, Gene Ontology: Tool for the unification of biology. *Nat. Genet.* **25**, 25–29 (2000).
111. T. G. O. Consortium; Gene Ontology Consortium, The Gene Ontology resource: Enriching a GOld mine. *Nucleic Acids Res.* **49**, D325–D334 (2021).
112. R. D. Finn *et al.*, Pfam: The protein families database. *Nucleic Acids Res.* **42**, D222–D230 (2014).
113. S. Lu *et al.*, CDD/SPARCLE: The conserved domain database in 2020. *Nucleic Acids Res.* **48** (D1), D265–D268 (2020).
114. D. H. Haft, J. D. Selengut, O. White, The TIGRFAMs database of protein families. *Nucleic Acids Res.* **31**, 371–373 (2003).
115. J. Huerta-Cepas *et al.*, eggNOG 5.0: A hierarchical, functionally and phylogenetically annotated orthology resource based on 5090 organisms and 2502 viruses. *Nucleic Acids Res.* **47** (D1), D309–D314 (2019).
116. J. J. Almagro Armenteros *et al.*, SignalP 5.0 improves signal peptide predictions using deep neural networks. *Nat. Biotechnol.* **37**, 420–423 (2019).
117. A. Krogh, B. Larsson, G. von Heijne, E. L. Sonnhammer, Predicting transmembrane protein topology with a hidden Markov model: Application to complete genomes. *J. Mol. Biol.* **305**, 567–580 (2001).
118. I. Lee, Y. Ouk Kim, S.-C. Park, J. Chun, A. N. I. Ortho, OrthoANI: An improved algorithm and software for calculating average nucleotide identity. *Int. J. Syst. Evol. Microbiol.* **66**, 1100–1103 (2016).
119. A. M. Eren *et al.*, Anvi'o: An advanced analysis and visualization platform for 'omics data. *PeerJ* **3**, e1319 (2015).
120. H. Hilgeri, M. Humer, Biotic landfill cover treatments for mitigating methane emissions. *Environ. Monit. Assess.* **84**, 71–84 (2003).
121. M. Mora *et al.*, Respirometric characterization of aerobic sulfide, thiosulfate and elemental sulfur oxidation by S-oxidizing biomass. *Water Res.* **89**, 282–292 (2016).
122. W. Martens-Habbena, P. M. Berube, H. Urakawa, J. R. de la Torre, D. A. Stahl, Ammonia oxidation kinetics determine niche separation of nitrifying Archaea and Bacteria. *Nature* **461**, 976–979 (2009).
123. Y. Perez-Riverol *et al.*, The PRIDE database and related tools and resources in 2019: Improving support for quantification data. *Nucleic Acids Res.* **47**, D442–D450 (2019).
124. S. F. Altschul, W. Gish, W. Miller, E. W. Myers, D. J. Lipman, Basic local alignment search tool. *J. Mol. Biol.* **215**, 403–410 (1990).
125. D. M. Emms, S. Kelly, OrthoFinder: Solving fundamental biases in whole genome comparisons dramatically improves orthogroup inference accuracy. *Genome Biol.* **16**, 157 (2015).
126. O. N. Kovalenko, N. N. Kundo, P. N. Kalinkin, Kinetics and mechanism of low-temperature oxidation of H_2S with oxygen in the gas phase. *React. Kinet. Catal. Lett.* **72**, 139–145 (2001).
127. C. Dahl, A. Prange, R. Steudel, "Metabolism of natural polymeric sulfur compounds" in *Miscellaneous Biopolymers and Biodegradation of Synthetic Polymers*, A. Steinbüchel, S. Matsumura, Eds. (Biopolymers, Wiley-VCH, Weinheim, Germany, 2002), vol. **9**, pp. 35–62.
128. J-H. Gwak *et al.*, Sulfur and methane oxidation by a single microorganism. NCBI GenBank. https://www.ncbi.nlm.nih.gov/nuccore/CP073764.1/. Deposited 1 April 2021.
129. J-H. Gwak *et al.*, Sulfur and methane oxidation by a single microorganism. NCBI GenBank. https://www.ncbi.nlm.nih.gov/nuccore/CP073765.1/. Deposited 1 April 2021.
130. J-H. Gwak *et al.*, Sulfur and methane oxidation by a single microorganism. ProteomeXchange. http://proteomecentral.proteomexchange.org/cgi/GetDataset?ID=PXD025979. Deposited 18 December 2021.
131. J-H. Gwak *et al.*, Sulfur and methane oxidation by a single microorganism. NCBI BioProject. https://www.ncbi.nlm.nih.gov/bioproject/PRJNA790002. Deposited 12 May 2021.